

# A Tyrosine Aminomutase from Rice (*Oryza sativa*) Isomerizes (*S*)- $\alpha$ - to (*R*)- $\beta$ -Tyrosine with Unique High Enantioselectivity and Retention of Configuration

Tyler Walter,<sup>†</sup> Zayna King,<sup>§</sup> and Kevin D. Walker<sup>\*,†,‡</sup>

<sup>†</sup>Department of Chemistry and <sup>‡</sup>Department of Biochemistry and Molecular Biology, Michigan State University, East Lansing, Michigan 48824, United States

<sup>§</sup>Medgar Evers College, Brooklyn, New York 11225, United States

## S Supporting Information

**ABSTRACT:** A recently discovered 3,5-dihydro-5-methylidene-4*H*-imidazol-4-one (MIO)-dependent tyrosine aminomutase (*O*<sub>s</sub>TAM) from rice [Yan, J., et al. (2015) *Plant Cell* 27, 1265] converts (*S*)- $\alpha$ -tyrosine to a mixture of (*R*)- and (*S*)- $\beta$ -tyrosines, with high (94%) enantiomeric excess, which does not change with pH, like it does for two bacterial TAMs. The  $K_M$  of 490  $\mu$ M and the  $k_{cat}$  of 0.005 s<sup>-1</sup> are similar for other TAM enzymes. *O*<sub>s</sub>TAM is unique and also catalyzes (*R*)- $\beta$ - from (*S*)- $\alpha$ -phenylalanine. *O*<sub>s</sub>TAM principally retains the configuration at the reactive C <sub>$\alpha$</sub>  and C <sub>$\beta$</sub>  centers during catalysis much like the phenylalanine aminomutase on the Taxol biosynthetic pathway in *Taxus* plants.

A class I lyase-like family of aminomutases (AMs) uses a 3,5-dihydro-5-methylidene-4*H*-imidazol-4-one (MIO) active site moiety to catalyze  $\alpha$ - to  $\beta$ -amino acid isomerization reactions. These catalysts are found on biosynthetic pathways to biologically active natural products that contain a  $\beta$ -amino acid building block.<sup>1–5</sup> The MIO facilitates the  $\alpha,\beta$ -elimination of the NH<sub>2</sub>/H pair from the  $\beta$ -aryl- $\alpha$ -amino acids and forms an NH<sub>2</sub>-MIO adduct, a tightly bound acrylate intermediate, and transfers a proton to a catalytic tyrosine.<sup>6</sup> As our knowledge of the stereochemical mechanism of MIO enzymes improves,<sup>1,3,7,8</sup> three subclasses begin to emerge. One class rotates the acrylate intermediate and places the *si* or *re* face toward the NH<sub>2</sub>-MIO. One rotamer rebounds back to the (*S*)- $\alpha$ -amino acid substrate, and the other commits to stereoselective catalysis of the (*R*)- $\beta$ -amino acid. After the acrylate rotates, the NH<sub>2</sub>/H pair rebound to the face of the acrylate opposite the one from which it was removed, resulting in retention of configuration (ROC) (Figure 1). A second subclass impedes the rotation of the acrylate, and the NH<sub>2</sub>/H pair rebounds to the face of the acrylate from which it was originally attached, proceeding with inversion of configuration (IOC) to make the (*S*)- $\beta$ -amino acid (Figure 1). Members of the third subclass, usually tyrosine aminomutases (TAMs), use both ROC and IOC mechanisms, making a mixture of (*R*)- and (*S*)- $\beta$ -tyrosines, typically with one enantiomer predominating.<sup>5</sup>

In a recent study, a tyrosine aminomutase from the monocot Japanese rice *Oryza sativa* (*O*<sub>s</sub>TAM) was shown to make exclusively (*R*)- $\beta$ -tyrosine.<sup>9</sup> No coumarate byproduct or (*S*)- $\beta$ -

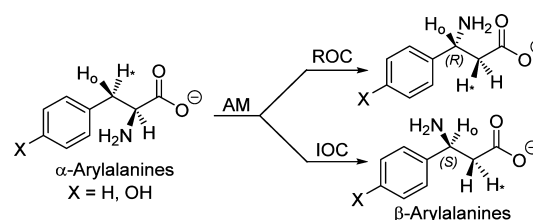


**Figure 1.** Exchange of the NH<sub>2</sub>/H pair by retention of configuration (ROC, top route) and inversion of configuration (IOC, bottom route).

tyrosine was observed in the earlier study, which is atypical for other TAMs and indicated a potential fourth subclass of MIO-AMs. Considering the preponderance of TAM catalysts that produce a mixture of enantiomers of  $\beta$ -tyrosine, herein, we reevaluated the product stereochemistry of *O*<sub>s</sub>TAM and reassessed whether *p*-coumarate is made as a byproduct.

Also, an earlier study showed that the enantiomeric ratio of  $\beta$ -tyrosine products changed with pH during catalysis by CcTAM from *Chondromyces crocatus*.<sup>8</sup> We describe the effects of pH on the enantiomeric ratio catalyzed by *O*<sub>s</sub>TAM. In addition, we calculated the intrinsic kinetic parameters of the recombinantly expressed enzyme and dissected the stereochemistry of the isomerization mechanism using stereospecifically <sup>2</sup>H-labeled tyrosines.

**Enzyme Expression and Assay.** *O*<sub>s</sub>TAM was cloned and expressed as an N-terminal His<sub>6</sub> fusion from the pET-28a(+) vector in *Escherichia coli* BL21 (DE3) cells. The enzyme (690 amino acids, 75 kDa) was purified (Ni-affinity and gel-filtration chromatographies) and concentrated by size-selective filtration (30 kDa molecular weight cutoff) to 1.8 mg/mL (~80% pure by SDS-PAGE and Coomassie Blue staining). After *O*<sub>s</sub>TAM (0.2 mg) had been incubated with (*S*)- $\alpha$ -tyrosine (1 mM) for 3 h, the reaction mixture was basified to pH 12, the tyrosines were converted to their 4'-*O*,3-*N*-di(ethoxycarbonyl) ethyl esters, and the *p*-coumarate byproduct was derivatized to its 4'-*O*-ethoxycarbonyl ethyl ester by the ethyl chloroformate and ethanol byproduct in the reaction. The derivatives were analyzed by gas chromatography/mass spectrometry (GC/EI-MS). The derivatized biosynthetic products had retention times and fragment ion abundances identical to those of authentic

Received: December 10, 2015

Published: December 28, 2015

standards derivatized equivalently (Figures S1–S5 and details in the Supporting Information). The  $k_{\text{cat}}$  of *OsTAM* was similar to those of other TAMs (*SgTAM*, *CcTAM*, and *KedY4*) yet ~10-fold slower than those of all phenylalanine aminomutases (PAMs) studied so far (Table S1). The  $K_M$  of *OsTAM* was similar in magnitude to those of *CcTAM* and *KedY4* and approximately 10-fold higher than those of all PAMs and one TAM (*SgTAM*). The equilibrium constant ( $K_{\text{eq}} \approx 1.1$  at 29 °C) at pH 9 is similar to that reported for three other MIO-aminomutases,<sup>3,10</sup> slightly favoring the  $\beta$ -isomer. Here, we found *OsTAM* does make *p*-coumarate, although slowly at 0.0017 s<sup>-1</sup>; this byproduct interestingly was not observed in a recent, independent study of *OsTAM*.<sup>9</sup>

#### Stereochemistry of the *OsTAM*-Catalyzed Reaction.

*OsTAM* was incubated with (2*S*)- $\alpha$ -tyrosine to assess the absolute stereochemistry and ratio of the  $\beta$ -tyrosine enantiomers produced by the biocatalyst. The amino acids in the reaction mixture were derivatized with chiral auxiliary (2*S*)-methylbutyric anhydride and diazomethane. The resulting 4'-*O*,3-*N*-di((2*S*)-methylbutyric) methyl esters were analyzed by GC/EI-MS (Figure S7). The biosynthetic  $\beta$ -tyrosines comprised a 97:3 mixture of *R* and *S* enantiomers; thus, *OsTAM*, like other TAMs, makes both enantiomers of  $\beta$ -tyrosine.

**Stereochemistry of NH<sub>2</sub>/H Rebound.** We used (2*S*,3*R*)-[3-<sup>2</sup>H]- and (2*S*,3*S*)-[2,3-<sup>2</sup>H<sub>2</sub>]- $\alpha$ -tyrosine<sup>8</sup> to assess the enantiospecific removal of the prochiral hydrogens at C $_{\beta}$  during *OsTAM* catalysis. *OsTAM* (0.2 mg) was incubated separately with each stereospecifically <sup>2</sup>H-labeled tyrosine for 3 h. Pyridine and ethyl chloroformate treatment gave the di(ethoxycarbonyl) <sup>2</sup>H-labeled amino acid ethyl esters that were analyzed by GC/EI-MS. Diagnostic fragment ions (Table S2) showed that the (3*R*)-<sup>2</sup>H of the 2*S*,3*R* substrate remained at the benzylic carbon of the  $\beta$ -product while the (3*S*)-<sup>2</sup>H of the 2*S*,3*S* substrate was transferred during the *OsTAM* reaction (Figure 2). Because the absolute configuration of the biosynthetic  $\beta$ -tyrosine is 3*R*, the NH<sub>2</sub> group thus adds to C $_{\beta}$  with ROC.

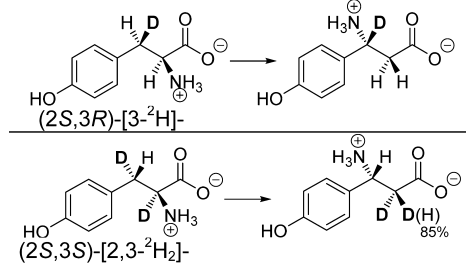


**Figure 2.** (2*S*,3*R*)-[3-<sup>2</sup>H]- and (2*S*,3*S*)-[2,3-<sup>2</sup>H<sub>2</sub>]- $\alpha$ -tyrosine substrates and the <sup>2</sup>H labeling of biosynthetic products inferred from GC/EI-MS analysis of *N,O*-diacyl ethyl ester derivatives. D-to-H exchange shown as a percentage.

The <sup>1</sup>H NMR chemical shifts of the prochiral hydrogens of the derivatized, authentic (*R*)- $\beta$ -tyrosine appear as an ABX spin system at  $\delta$  2.89 (dd, <sup>2</sup>*J* = -15 Hz; <sup>3</sup>*J* = 6.0 Hz) and  $\delta$  2.78 (dd, <sup>2</sup>*J* = -15 Hz; <sup>3</sup>*J* = 6.0 Hz) (Figure 3A). (2*S*,3*R*/2*R*,3*S*)-[2,3-<sup>2</sup>H<sub>2</sub>]- $\beta$ -Tyrosine (81% dideuterio; 88% D at C $_{\alpha}$ ; 92% D at C $_{\beta}$ ) was synthesized by Pd-catalyzed *syn* addition of D<sub>2</sub> gas to methyl (*Z*)-*N*-acetamido-(4-methoxyphenyl)acrylate. The chemical shift singlet for the lone C $_{\alpha}$ -H of the derivatized racemic mixture of [2,3-<sup>2</sup>H<sub>2</sub>]- $\beta$ -tyrosine appeared at  $\delta$  2.88 (Figure 3B). The C $_{\alpha}$ -H of the latter dideuterio racemate is

*gauche* to the  $\beta$ -acetamido in a staggered *anti* conformation when the phenyl ring and carboxy ester groups are farthest apart. This infers that the  $\delta$  2.89 (dd) resonance of the perproton (*R*)- $\beta$ -tyrosine corresponds to the *pro*-2*R* hydrogen and the one at  $\delta$  2.78 corresponds to the *pro*-2*S* hydrogen (Figure 3A).

To assess the stereochemistry of the hydrogen rebound, [3,3-<sup>2</sup>H<sub>2</sub>]- $\alpha$ -tyrosine (5 mM) was incubated with *OsTAM* (5 mg) in 20 mM phosphate buffer (pH 9.0) at 29 °C for 6 days. The isotopomers in the mixture were derivatized to their (4'-*O*-methyl,*N*-acetyl) methyl esters, dissolved in CDCl<sub>3</sub>, and analyzed by <sup>1</sup>H NMR. One derivatized biosynthetic <sup>2</sup>H-labeled  $\beta$ -tyrosine isotopomer had proton resonances at  $\delta$  2.89 (d, <sup>2</sup>*J* = -16 Hz) and  $\delta$  2.78 (d, <sup>2</sup>*J* = -16 Hz) (Figure 3C). The <sup>1</sup>H NMR data are consistent with a diprotio-CH<sub>2</sub> of a [3-<sup>2</sup>H]-(*R*)- $\beta$ -tyrosine isotopomer, present at 77% relative to a second isotopomer, which we identified as (2*S*,3*R*)-[2,3-<sup>2</sup>H<sub>2</sub>]- $\beta$ -tyrosine (23% abundant). The latter had a single resonance at  $\delta$  2.88 (singlet) for the single proton on the methylene carbon. GC/EI-MS analysis of the derivatized biosynthetic  $\beta$ -tyrosine confirmed the ratio of mono- and dideuterio isotopomers (Figure S21). Together, these <sup>1</sup>H NMR data suggest that *OsTAM* migrates the deuterium from C $_{\beta}$  of [3,3-<sup>2</sup>H<sub>2</sub>]- $\alpha$ -tyrosine to the *pro*-*S* position at C $_{\alpha}$  of  $\beta$ -tyrosine with 23% deuterium retention and 77% D-to-H exchange (Figure 3C). This D-to-H exchange was similarly observed for a *TcPAM*<sup>3</sup> and *CcTAM*.<sup>8</sup> Thus, *OsTAM* catalyzes its isomerization reaction with ROC at each reactive carbon center (Figure 1).

**Effect of pH on the Stereochemistry of  $\beta$ -Tyrosine Catalyzed by *OsTAM*.** In previous studies of other tyrosine aminomutases, *SgTAM*<sup>11</sup> and *CcTAM*,<sup>8,12</sup> the *R*:*S* ratio of  $\beta$ -tyrosine enantiomers biosynthesized by each catalyst changed as the reactions progressed.<sup>5</sup> The earlier study of *CcTAM* showed that at pH 7 the amount of (*S*)- $\beta$ -tyrosine relative to the *R* isomer increased from 10 to 20% as the conversion of  $\alpha$ - to  $\beta$ -tyrosine progressed from 13 to 55%, respectively. The latter study also showed that as the pH increased from 7 to 9 the (*S*)-antipode increased from 10 to 17% after 13% conversion of the  $\alpha$ - to  $\beta$ -amino acid and from 20 to 27% after 55% conversion, respectively.<sup>8</sup> These earlier data strongly suggested that the enantiomeric ratio of the products catalyzed by TAMs is likely dependent on pH and reaction progress. To assess the effects of pH on *OsTAM*, (2*S*)- $\alpha$ -tyrosine was incubated with *OsTAM* for 24 h at pH 7, 8, 9, and 10. *OsTAM* interestingly maintained an ~97:3 *R*:*S* ratio as the reaction reached different maximal conversions (9–52% conversion of  $\alpha$ - to  $\beta$ -tyrosine) for each reaction at pH 7–10 over 24 h (Figure 4). The dearth of (3*S*)-antipode (~3%) catalyzed by *OsTAM* might have contributed to it being overlooked in an earlier study that used HPLC separation and fluorescence detection of the product.<sup>9</sup>

**Comparing the Active Sites of MIO-Dependent Enzymes.** Similar to those of other MIO-dependent AMs, the *OsTAM* active site comprises residues from three monomeric subunits of the active homotetramer.<sup>4,13,14</sup> An Ala-Ser-Gly triad forms the MIO group; a catalytic Tyr98 is poised to transfer a C $_{\beta}$  hydrogen of the substrate, and a conserved Arg344 is positioned to form a carboxylate salt bridge with the substrate. *OsTAM* catalyzes its product with similar *R* enantioselectivity (~97%) as *TcPAM*, catalyzing its reaction with a 99.9% preference for (*R*)- $\beta$ -phenylalanine.<sup>15</sup>

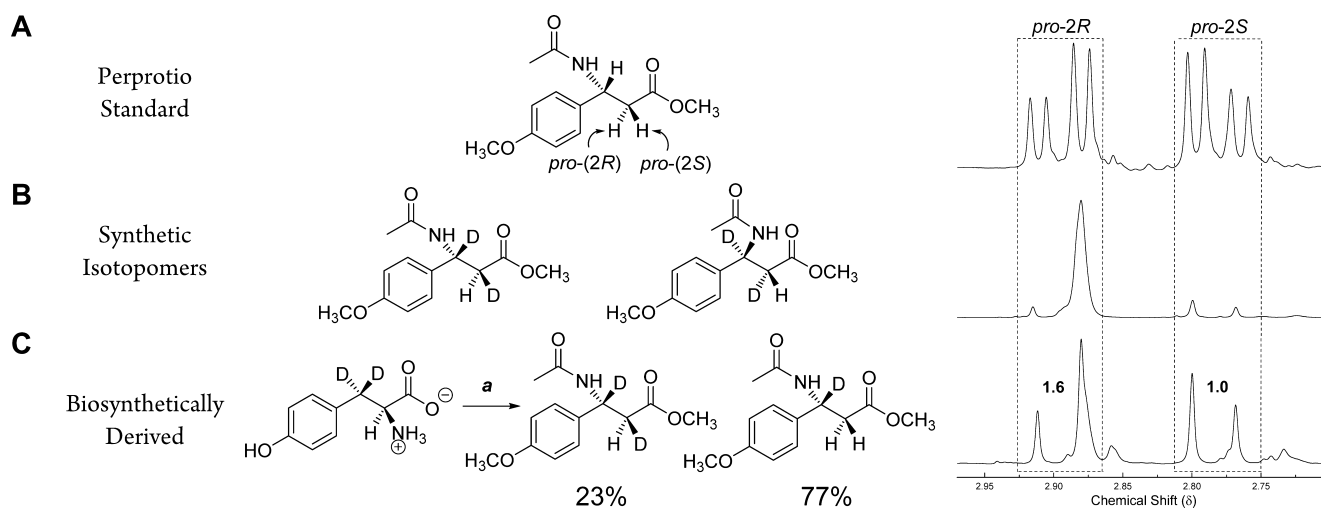


**Figure 3.** Partial  $^1\text{H}$  NMR spectra of 4'-*O*-methyl,*N*-acetyl methyl ester derivatives of  $\beta$ -tyrosine isotopomers. Chemical shifts of (A) the prochiral hydrogens of derivatized authentic  $\beta$ -tyrosine, (B) the  $\text{C}_\alpha$  hydrogen of derivatized authentic (2*S*,3*R*/2*R*,3*S*)-[2,3- $^2\text{H}_2$ ]- $\beta$ -tyrosine (81% dideuterio), and (C) the  $\text{C}_\alpha$  hydrogens of derivatized biosynthetic  $\beta$ -tyrosine catalyzed by *Os*TAM. (a) (i) *Os*TAM; (ii) base, acetic anhydride; (iii) HCl; (iv)  $\text{CH}_2\text{N}_2$ . Numbers in NMR spectrum are relative peak areas.

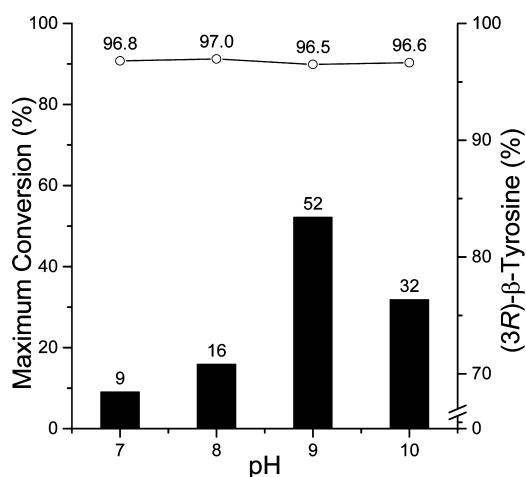


**Figure 4.** Maximal conversion of  $\alpha$ -tyrosine to the 3*R*  $\beta$ -isomer catalyzed by *Os*TAM over 24 h from pH 7 to 10 (black bars). Percent of biosynthetic (3*R*)- $\beta$ -tyrosine made by *Os*TAM relative to the (3*S*)-antipode (○).

Comparing a structural model of *Os*TAM and the *Tc*PAM structure (PDB entry 3NZ4) shows several shared residues surrounding their active sites (Figure 5). The active site residues of these plant-derived aminomutases differ by only two residues. These striking similarities likely explain their shared enantioselective bias for the *R* enantiomer. However, *Os*TAM uses a Tyr125/Asn446 pair, while *Tc*PAM uses Cys107/Lys427 partners positioned similarly near the *para* carbon of the phenylpropanoid substrates. These functionally distinct residues likely define their respective substrate selectivities. The Tyr125(*Os*TAM) residue likely engages in a H-bonding interaction with the 4'-hydroxyl of the tyrosine substrate. The longer reach of the H-bonding Tyr125(*Os*TAM) residue over the shorter Cys107(*Tc*PAM) likely allows *Os*TAM to interact better with its tyrosine substrate. By contrast, Cys107 of *Tc*PAM likely H-bonds with its Lys427 partner, helping to construct a hydrophobic active site pocket to instead bind phenylalanine. The use of an extended length, polar residue (such as Tyr125) by *Os*TAM to confer its substrate selectivity

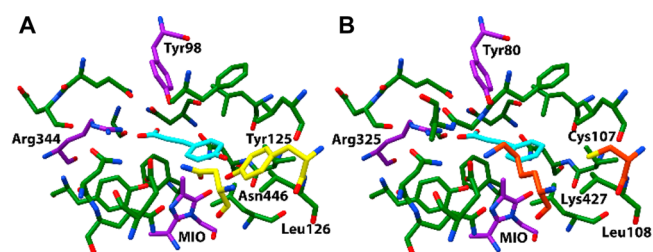


**Figure 5.** Active sites of (A) *Os*TAM structure model and (B) *Tc*PAM (PDB entry 3NZ4). Residues common to both enzymes (green), the catalytic Arg and Tyr residues, and the MIO (purple) are depicted. Asn446 and Tyr125 (yellow) near the *para* carbon of the coumarate intermediate modeled in *Os*TAM are depicted; equivalently positioned residues (orange) near the *para* carbon of cinnamate in complex with *Tc*PAM are also shown. Heteroatoms: oxygen (red), nitrogen (blue), and sulfur (yellow).

for tyrosine is supported by an earlier study of a *Tc*PAM homologue (*Tch*PAM from *Taxus chinensis*).<sup>16</sup> In the earlier study, the further-reaching Cys107His mutation allowed *Tc*PAM to turn over tyrosine with high enantioselectivity,<sup>16</sup> suggesting that His107 formed a selective interaction with the 4'-hydroxyl of the tyrosine substrate.

**Substrate Selectivity of *Os*TAM.** All known TAMs use a 3-(4-hydroxyaryl)alanine substrate, while PAMs use phenylalanine derivatives and preclude tyrosine as a substrate. TAMs typically use polar residues (Ser, His, Glu/Thr, and Tyr) near the 4'-hydroxyphenyl ring of the tyrosine substrate (Figure 6). In contrast, PAMs use a mixture of variously hydrophobic and polar residues (Ala/Cys, Val/Leu, Met/Lys, and Ile/Phe) near the phenyl ring of the eponymous substrate.

*Os*TAM uses a combination of polar and hydrophobic residues (Tyr125, Leu126, Asn446, and Val450) around the aryl ring of the substrate that resemble those found in PAMs more than in TAMs. Therefore, (*S*)- $\alpha$ -phenylalanine was incubated with *Os*TAM to test its PAM activity. The biosynthesized products were *N,O*-derivatized and analyzed by GC/EI-MS as before. *Os*TAM slowly converted ( $k_{\text{cat}}^{\text{APP}} = 0.00017 \text{ s}^{-1}$ ) (*S*)- $\alpha$ - to (3*R*)- $\beta$ -phenylalanine with a  $K_M^{\text{APP}}$  of 9 mM (Figures S32 and S33), thus marking the first instance of a

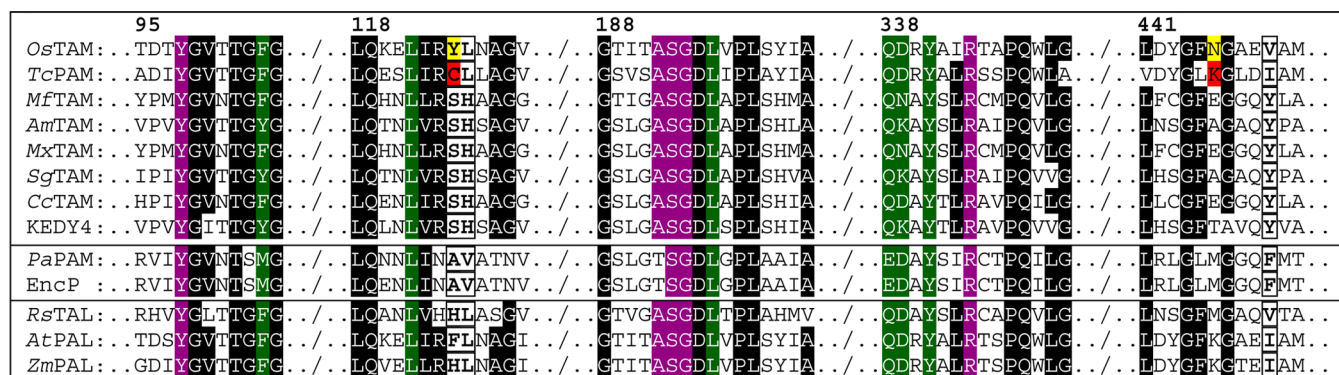


**Figure 6.** Partial sequence alignment (GeneDoc) of MIO-dependent enzymes. Conserved residues (highlighted in purple) are catalytic Tyr, Arg (binds the carboxylate of the substrate), and the Ala/Thr-Ser-Gly triad (form the MIO cofactor). Isosterically similar residues in the active site of MIO catalysts (highlighted in green) and residues near the *para* carbon of the substrate in TcPAM (highlighted in red) and OsTAM (highlighted in yellow). Residues proposed as being key for substrate selectivity are bold and boxed. Identical residues shared in 10 of the 13 sequences (highlighted in black). Residue numbering based on OsTAM. Accession numbers are in the [Supporting Information](#).

wild-type aminomutase that uses both  $\alpha$ -phenylalanine and  $\alpha$ -tyrosine as substrates.

This study adds information about the mechanisms of catalysis of MIO-dependent aminomutases. Here, we find, like two other TAMs (CcTAM and SgTAM), OsTAM catalyzes a mixture of (*R*)- and (*S*)- $\beta$ -tyrosine, but with very high enantioselectivity ( $\sim 97\%$ ) for the *R* isomer. By contrast, three other bacterial TAMs are reported to catalyze exclusively the (*S*)- $\beta$ -amino acid.<sup>5,17</sup> The enantiomeric ratio catalyzed by OsTAM is virtually unaltered by pH and reaction progress, unlike those of bacterial SgTAM and CcTAM, whose *R*:*S* ratios vary over time.<sup>7,8,12</sup> This investigation provides a basis to begin inquiry into how the rice OsTAM restricts its enantioselectivity. Further, after defining the absolute stereochemistry and using <sup>2</sup>H-labeled tyrosines, we showed that the OsTAM mechanism principally retains the configuration at C <sub>$\alpha$</sub>  and C <sub>$\beta$</sub>  after the isomerization. This reaction pathway is similar to the mechanism followed by TcPAM, also from a plant. The unique active site residues of OsTAM are more permissive than those in TcPAM and allow OsTAM to turn over two aromatic amino acids, although with a substantial preference for tyrosine. As more MIO aminomutases are discovered and their cryptic stereochemistries examined, a new subdivision of MIO-dependent enzymes that distinguishes plant aminomutases from those in bacteria might emerge.

## ■ ASSOCIATED CONTENT

### 📄 Supporting Information

The Supporting Information is available free of charge on the [ACS Publications website](#) at DOI: [10.1021/acs.biochem.5b01331](https://doi.org/10.1021/acs.biochem.5b01331).

Experimental methods, GC/MS and NMR data, and gene accession numbers ([PDF](#))

## ■ AUTHOR INFORMATION

### Corresponding Author

\*E-mail: [walker@chemistry.msu.edu](mailto:walker@chemistry.msu.edu).

### Funding

The authors are grateful to the MSU Office for Inclusion and Intercultural Initiatives for supporting the MSU Chemistry 4-Plus Bridge to the Doctorate Program (Z.K., GA017081-CIEG).

## Notes

The authors declare no competing financial interest.

## ■ ACKNOWLEDGMENTS

We thank undergraduate Devinda Wijewardena for his technical assistance.

## ■ REFERENCES

- (1) Ratnayake, N. D., Wanninayake, U., Geiger, J. H., and Walker, K. D. (2011) *J. Am. Chem. Soc.* 133, 8531–8533.
- (2) Magarvey, N. A., Fortin, P. D., Thomas, P. M., Kelleher, N. L., and Walsh, C. T. (2008) *ACS Chem. Biol.* 3, 542–554.
- (3) Mutatu, W., Klettke, K. L., Foster, C., and Walker, K. D. (2007) *Biochemistry* 46, 9785–9794.
- (4) Christianson, C. V., Montavon, T. J., Van Lanen, S. G., Shen, B., and Bruner, S. D. (2007) *Biochemistry* 46, 7205–7214.
- (5) Krug, D., and Müller, R. (2009) *ChemBioChem* 10, 741–750.
- (6) Wanninayake, U., and Walker, K. D. (2012) *Biochemistry* 51, 5226–5228.
- (7) Christianson, C. V., Montavon, T. J., Festin, G. M., Cooke, H. A., Shen, B., and Bruner, S. D. (2007) *J. Am. Chem. Soc.* 129, 15744–15745.
- (8) Wanninayake, U., and Walker, K. D. (2013) *J. Am. Chem. Soc.* 135, 11193–11204.
- (9) Yan, J., Aboshi, T., Teraishi, M., Strickler, S. R., Spindel, J. E., Tung, C. W., Takata, R., Matsumoto, F., Maesaka, Y., McCouch, S. R., Okumoto, Y., Mori, N., and Jander, G. (2015) *Plant Cell* 27, 1265–1278.
- (10) Chesters, C., Wilding, M., Goodall, M., and Micklefield, J. (2012) *Angew. Chem., Int. Ed.* 51, 4344–4348.
- (11) Christenson, S. D., Wu, W., Spies, M. A., Shen, B., and Toney, M. D. (2003) *Biochemistry* 42, 12708–12718.
- (12) Rachid, S., Krug, D., Weissman, K. J., and Muller, R. (2007) *J. Biol. Chem.* 282, 21810–21817.
- (13) Feng, L., Wanninayake, U., Strom, S., Geiger, J., and Walker, K. D. (2011) *Biochemistry* 50, 2919–2930.
- (14) Strom, S., Wanninayake, U., Ratnayake, N. D., Walker, K. D., and Geiger, J. H. (2012) *Angew. Chem., Int. Ed.* 51, 2898–2902.
- (15) Klettke, K. L., Sanyal, S., Mutatu, W., and Walker, K. D. (2007) *J. Am. Chem. Soc.* 129, 6988–6989.
- (16) Wu, B., Szymanski, W., Wijma, H. J., Crismaru, C. G., de Wildeman, S., Poelarends, G. J., Feringa, B. L., and Janssen, D. B. (2009) *Chem. Commun.* 46, 8157–8159.
- (17) Van Lanen, S. G., Oh, T.-j., Liu, W., Wendt-Pienkowski, E., and Shen, B. (2007) *J. Am. Chem. Soc.* 129, 13082–13094.